Phase Discrimination in Marine Icing Using a Coplanar Capacitive Array

Abdulrazak Elzaidi, Vlastimil Masek, and Yuri Muzychka

***Abstract*— This paper describes the development of an array of coplanar capacitive sensors applied to marine icing. Current atmospheric icing monitoring systems consider single phase conditions in their operation. Marine icing conditions present a unique environment where the liquid water phase effects cannot be neglected and require a novel approach. We have conducted an initial proof of concept and propose a new icing monitoring system which can distinguish between the individual phases. A numerical model confirmed our initial hypothesis of the system's ability to discriminate the multiphase domains based on the array of geometrically dissimilar capacitive sensors. In addition, we also developed a novel experimental technique based on a comparative study under constant conditions to eliminate the need for an independent ice accretion monitoring system normally required in sensor development. The new approach promises a better characteristic in marine icing monitoring systems or in similar applications where multiphase dielectric is present.**

***Index Terms*— Capacitive sensors, multiphase dielectric material, coplanar electrodes, finite element analysis, capacitance-to-frequency conversion, linearly independent characteristics, least squares equations, offshore industry, wind power generation, marine icing.**

I. Introduction

NEW methodology for monitoring marine icing phenomena in arctic offshore environments is being proposed. Marine icing is created by a combination of low air temperatures and water spray and can severely affect ships or offshore platforms [1]. Offshore wind farms can face a reduced efficiency due to the ice accretion. For example, the icing can lead to the rotor imbalance which can lead to the system being permanently damaged [2].

The ice layer in marine icing is formed when super-cooled water spray droplets freeze on parts of the structure before the water runoff time elapses [3], [4]. A number of laboratory derived methods to monitor the icing has been proposed recently such as the systems based on image processing in visible or IR light in [5]–[8]. These are complex systems and require an unobstructed view, artificial ambient lighting, possibly camera vibration damping besides other requirements which makes their deployment in the harsh marine environment challenging and maintenance costly.

Manuscript received June 21, 2019; revised August 9, 2019; accepted August 11, 2019. Date of publication August 15, 2019; date of current version November 13, 2019. The associate editor coordinating the review of this article and approving it for publication was Prof. Tarikul Islam. *(Corresponding author: Abdulrazak Elzaidi.)*

The authors are with the Faculty of Engineering and Applied Science, Memorial University of Newfoundland, St. John's, NL A1B 3X5, Canada (e-mail: abdoeziedy@ieee.org).

Digital Object Identifier 10.1109/JSEN.2019.2935616

Sensors of low cost characteristic, robust performance and low maintenance are preferred by the industry. The need for expert installation or field re-calibration is additional factor considered in this research. Deployment on a curved rotor blade requires a low weight characteristic and ability of being integrated on a curved surface. Battery operation in wirelessly connected systems require low power characteristics. We have considered a number of existing techniques with these requirements in mind and developed a new method along a proof-of-concept prototype for experimental validation.

A range of ideas was adopted in our development at an individual sensor level before we combined an array of dissimilar geometry capacitive sensors to decode two layers of ice and water uniquely. We developed a novel data analysis based on least squares equations to generate a formula of signal-to-measurand mapping.

A comparative study without the need for an expensive experimental setup with an independent ice monitoring system proved the new concept's feasibility. This presented research work outlines the first step in our icing sensor development and provides a level of confidence needed for the further study.

The next Section II outlines the background information in the field of icing sensing in general and capacitance, followed by Section III which describes a theoretical approach to pre-validate the new concept. Section IV explains the hardware setup to conduct the experimental work with results in Section V. Conclusions are drawn in Section VI followed by Acknowledgement and References.

II. Previous Work

A large proportion of the current literature on icing sensing systems considers atmospheric icing phenomena on land that also causes severe operational and safety hazards to personnel or equipment like power distribution systems, wind power generation systems, cable cars, transportation or communication towers. A comprehensive survey of current commercial systems is presented in [2].

A research team from Graz Technical University [9] describes their latest work on using a capacitive array applied to atmospheric icing on high voltage power lines. The objectives are somewhat similar, however the sensor array composition and the signal processing methods are different. Their method is using a larger size array with a constant spacing and constant spatial distribution which enables a computer tomography type analysis to assess irregularities in ice accretion across the sensed area. Our system considers a relatively

small size array to monitor a localized area. Similarly to our work, Graz team considered the two phase phenomena, ice and water. What makes our independent research largely different is the location of the water domains. We focus more on the surface water layer above the ice while the referenced work considers water domains trapped in the ice layer once the ice starts forming. The lack of common experimental data (marine vs atmospheric) makes it difficult to compare both methods.

On the commercial side, Combitech IceMonitor [10] measures the ice mass on a rotating rod by a load cell. One of the best systems on the market for terestrial applications there is a need for keeping the rotating parts such as bearings free of ice in case of severe conditions. The system provides accuracy of $\pm 50g$ and is not used for measuring light icing events. The system requires a stationary installation which could challenge a potential use in marine/offshore applications due to the dynamic forces, vibration, wind gusts or dynamic water splashes. A long term stability issues have been addressed in [2].

The Goodrich 0871LH1 ice detectors [11] use an axially vibrating probe to detect the presence of icing conditions. In an icing environment, ice collects on the sensing probe, causing the resonance frequency of the sensing probe ($\sim$40 kHz) to decrease. The ice load depends linearly on the induced frequency shift. When the ice accretion increases beyond a predefined threshold, the probe is de-iced until the frequency rises back to the normal conditions. Goodrich ice detector is designed for thin ice layer applications like avionics and to the date no reports of detecting the ice under the water phase presence has been released.

HoloOptics T42 [12] employs IR signal passed through the medium between the emitter and the detector. In heavy intensity rain or dew the probe may saturate, resulting in a false indication. The manufacturer recommends using an external rain detector together with the sensor to eliminate the sources of false indications. No testing in marine icing conditions was conducted with the T42.

The Ice Meister Model 9734-SYSTEM industrial ice detector [13] monitors the optical characteristics of the substance which is in contact with the optical surfaces of the probe. The parameters measured are opacity and optical refraction. This sensor has no specified accuracy, and is not intended to be used as an analog measuring instrument of any kind. It only recognizes whether air, water or ice is present. This concept is somewhat similar to chilled mirror dew point sensor which often employs the optical reflectivity.

IDS-20 system [14] measures the complex impedance of the icing medium using capacitive plates hermetically sealed. The sensor can distinguish between water and ice as the above sensor, however not in a combined multiphase state.

Zhi et al. [15] conducted recently an experimental research using capacitive sensors to measure ice growth in real time. The developed system has also been patented [16] but the authors conclude the water layer formation has to be prevented in order to maintain the accuracy. Ezeoru [17] conducted a similar research using the same capacitive technique with interdigitated comb-style electrodes. Both works experienced the transformation from liquid state to solid state which has been reflected in a ramp capacitance profile in time. However, no one has tried to quantify the transitional multiphase period.

A. Capacitive Sensing

Capacitive sensors are widely used in many industrial and scientific applications due to their simplicity, low cost, high reliability, long term stability and simple signal conditioning [18]. In our application, the sensor features a low profile design that can be attached to flat or curved surfaces. In addition, a simple de-icing mechanism can be conveniently integrated on the same substrate like in a car windshield defogging system. The capacitive probe is usually lightweight, making the sensor suitable for placement on dynamic systems or moving parts.

A capacitor in a charged state creates an electric field that is modulated by the presence of a dielectric material in its proximity. In many applications, the electric field is distributed across the measured dielectric material while being confined between two sensing plates of a regular shape. Most frequently, the field eqipotential lines are parallel or concentric with the electrodes in which case an analytical modeling in a curvilinear coordinate system can be very accurate.

Our method exploits the concept of fringing fields set by a coplanar pair of electrodes. Planar capacitors can take many different shapes and forms like interdigitated (comb fingers), rectangular or circular spirals etc. Ezeoru [17], Go [16], Arshak [19] used the interdigitated electrodes while Gong [20] and Chen [21] used spiral electrodes. Whichever form the planar capacitor takes, the common key parameter is the dimension of the gap along the interfacial line between the two electrodes. As long as the covered sensing area is the same, all geometries are equivalent and it is only the matter of a personal choice.

Capacitive sensors are however prone to undesired effects of parasitic and offset capacitances as well as the dielectric loss in the form of a conductance. Our capacitive array is spin coated to form an insulation layer to significantly suppress the effect of the conductance and a simple capacitance to frequency conversion is being employed. However, more advanced and very accurate conversion methods have been recently developed like the research of Malik et al. [22] where the maximum error due to parasitic capacitance is found to be within $\pm 0.05\%$.

Our method also operates on a differential principle in which four capacitances are compared by an algorithm. This concept can be viewed as a multidimensional Wheatstone bridge. In general the comparative or differential methods are very effective to deal with the offset and parasitic capacitance as long as they drift consistently, in most cases due to temperature effects. A brief analysis of the drift effects is presented in the Results section.

The work of Alex Risos [23]–[26] on interdigitated capacitive sensors employs the differential principle in which the reference sensor is thermally coupled with the transformer oil sensing probe. He also uses a four wire bridge measurement technique which significantly suppresses the effect of lead wire impedance. Risos et al also points out another potential issue surrounding the capacitive sensors which is a noise source by

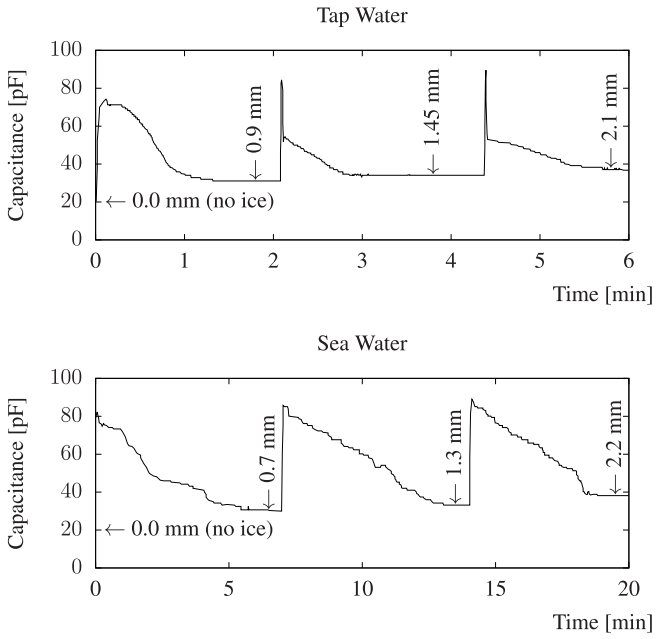

Fig. 1. Experiment for Sensor Calibration, Ezeoru 2016 [17].

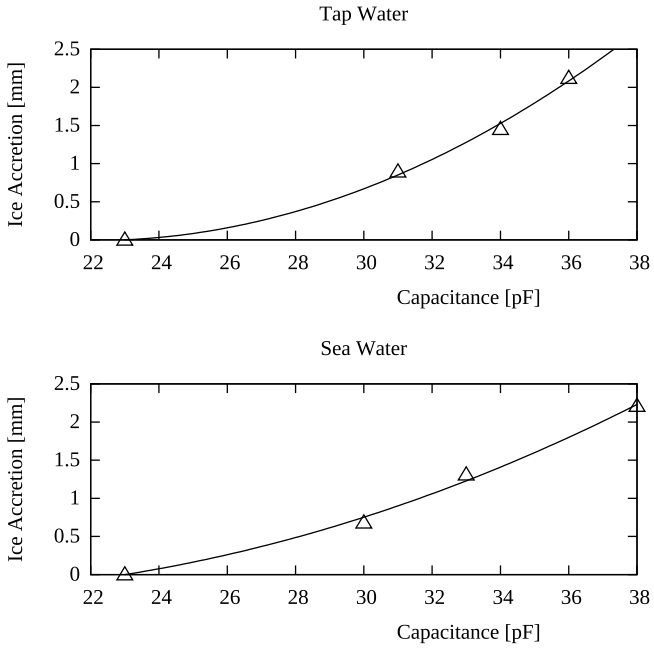

Fig. 2. Ice Accretion vs Capacitance.

charged particles in the dielectric medium being analyzed. To eliminate the effect of such charges and the parasitic capacitance, he introduced a liquid permeable Faraday cage above the sensor plain plus inserted a tiny deflector electrode between the sensing electrodes. The deflective electrode is held at the GND potential but is not connected to GND. Unfortunately we cannot use this method as any cage in front of the sensor would be subject to the icing phenomena. Heating the Faraday cage would not be effective either as the thermodynamic balance would be negatively affected. In our research however, we do not anticipate any charged particles in the dielectric medium since each conductive droplet arriving at the sensor plain originates from the ocean wave breaking off the ship bow which are in fact the GND reference. To our knowledge there is also no mechanism of acquiring a charge during the flight through moist atmosphere above the ocean. In terms of the deflector electrode, we may introduce this technique in the future work. Currently our sensor array is using a variation in the gap between the electrodes which prohibits the deflector electrode use without a modified approach.

Figure 1 shows experimental data acquired by Ezeoru [17] at a rate of 16 samples per second, or $\sim$ 1000 samples per 1 minute. The graph describes ice forming in three transitional steps (water to ice), tap water on top and sea water below. Each step starts by wetting the sensor plane and waiting for the water to turn into ice at a constant $-20°C$. One can observe that the sea water of 3.5% salinity (by mass) takes much longer to turn into ice. The ice accretion was determined by weight measurement.

From [17] we extracted four pairs of data as indicated by arrows in Figure 1 in order to derive the calibration characteristics for low ice accretion levels shown in Fig. 2.

The capacitance data were first normalized according to (1) and then utilized in least squares fitting of a quadratic characteristic (2) as depicted in Figure 2. The fitting was derived with the final sum of squares of residuals of 0.00869474 as

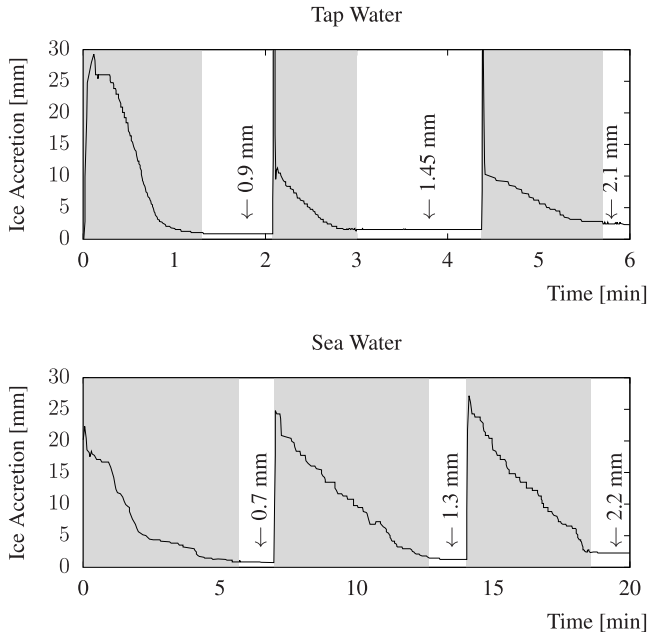

Fig. 3. Faulty Measurement Results under Two-Phase Conditions.

compared to 0.146793 in a liner characteristic fit (tap water case).

Applying the single phase icing sensor characteristic to the original two-phase conditions during the transients we generated Figure 3. The grey segments are subject to errors of the order of magnitude which limits the sensor's application in two-phase marine icing conditions.

Applying this technique to marine icing would require a human operator to extract the bottom envelope of the measurement data and disregard the multiphase transients that provide faulty ice accretion reading. This is feasible in a lab derived data however real marine icing conditions make this human intervention task difficult as there may never be a period of

TABLE I
ANSYS MAXWELL MODEL PARAMETERS

tag	object	material	ε_r	sources	matrix
Ⓐ	background	air	1.0006		
Ⓑ	balloon			voltage	
Ⓒ	object2	water-fresh	81		
Ⓓ	object1	ice	4.2		
Ⓔ	electrode-gnd	copper		0V	GND
Ⓕ	electrode-sig	copper		1V	Signal
Ⓖ	dielectric	epoxy-Kevlar-xy	3.6		
Ⓗ	PCB-backing	epoxy-Kevlar-xy	3.6		

single phase icing for a period of time when the sensor is constantly exposed to icy waters. Also applying a low pass filter with a low corner frequency would smooth the transients at the cost of raising the bias making the data unreliable again. Therefore, unless single phase conditions can be guaranteed, we need to consider the effects of both water and ice together.

$$\hat{C} = \left(\frac{C - \bar{C}}{\bar{C}}\right) \tag{1}$$

$$h = k_1\hat{C} + k_2\hat{C}^2 \tag{2}$$

h	[mm] ice accretion
$\hat{C}$	[1]normalized capacitance
C	[pF] measured capacitance
$\bar{C}$	[pF] nominal capacitance
k_1, k_2	[mm] constant coefficients

III. FEM SIMULATION

The marine icing phenomena as described above consists of both the solid phase (ice) and the liquid phase (water) with a different proportion at different times. Except [9], all known methods assume only the ice phase which makes it inaccurate if the water phase is present as there is a large discrepancy in the dielectric constant between the ice and water ($\sim 20\times$).

We adopted a concept of modulating the sensor's depth of penetration by changing the air gap between two spiral electrodes, [21], [27]. Two different electrode separation sensors uniquely modulate the electric field above the XY plane of each sensor. The resulting capacitances must therefore be linearly independent of each other making it possible to discriminate between the two phases.

In order to verify the above statement, we first conducted a finite element simulation using two concentric electrode probes of 1mm and 2mm electrode separation in a similar way as described in [21], [27]. The problem was modeled in Maxwell software developed by Ansys using axisymmetrical coordinates in RZ plane. Table I lists all domains in the model and their corresponding parameters.

The capacitance is calculated from the total field energy W across the modeling domain using 3 where V represents the applied voltage, conveniently set to 1V for easier result validation.

$$C = \frac{2W}{V^2} \tag{3}$$

The field for the sensor geometry having 2mm electrode separation and r = 9mm & R = 15mm is depicted in Figure 4. The second geometry has 1mm separation and r = 10mm & R = 15mm. When two characteristics are linearly independent, a common solution can be derived from their intersection point. Figure 5 demonstrates this concept using contours of constant capacitance for the two sensor geometries combined in one plane, 1mm sensor contours depicted by solid lines and 2mm sensor contours by dashed lines. One particular solution is highlighted for 1mm gap sensor at 6.5pF capacitance and 2mm gap sensor at 5.0pF capacitance having a common intersection point at 0.75mm ice layer and 0.35mm water layer above. The larger the angle of intersection between any two contours the more robust solution is derived. This type of analysis was conducted by Ortiz [31].

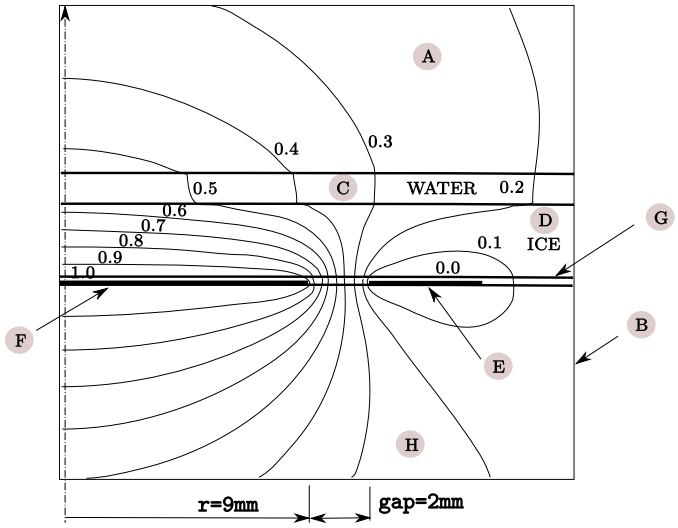

Fig. 4. Equipotential Lines of Electric Field for 2.5mm Ice&1mm Water.

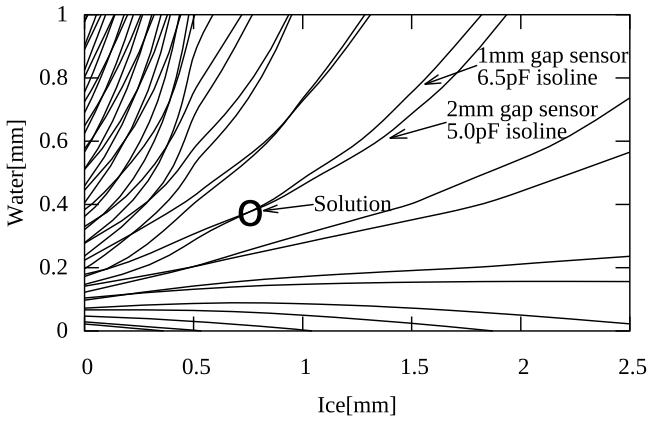

Fig. 5. Contours of Constant Capacitance for Both Sensor Geometries.

In summary, the FEM simulations have proven in theory that an array of coplanar sensors of different electrode spacing characteristics can uniquely map the presence of the water phase and use this information in deriving the ice accretion level with more accuracy and confidence.

IV. EXPERIMENTAL SETUP

Chen and Bowler [21], [27] used a simple PCB layout software approximating the spiral electrodes by arc segments

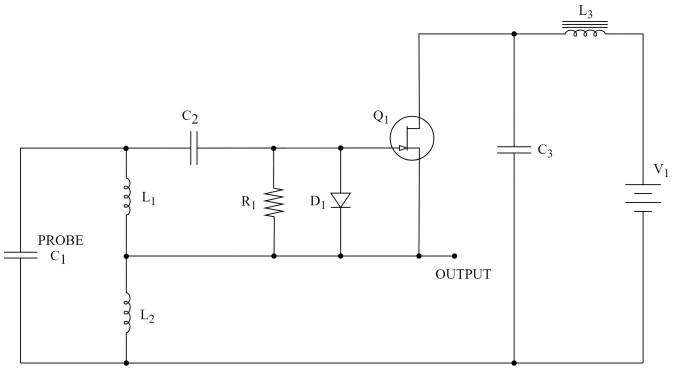

Fig. 6. Hartley Oscillator as Capacitance-to-Frequency Converter.

of varying radii creating a small discontinuity whenever two 180° arc segments of different radii are connected. Our array of capacitive probes was manufactured on a printed circuit board (PCB) with the spiral electrodes modeled by OpenSCAD software as true Archimedes spirals ensuring a constant spacing between each electrode pair.

The PCB was spin coated with a thin layer of dielectric lacquer to eliminate the effect of conductivity between the individual electrodes. A similar process is widely used in many commercial systems such as tactile/touch sensor from Texas Instruments [29].

Each probe is conditioned by a capacitance-to-frequency converter which utilizes FET Hartley oscillator, Figure 6. The air-core coil is provided with a center tap and was made using a *basket weave* technique to suppress a parasitic capacitance and a magnetic coupling via the proximity effect. We have subjected each channel to two extreme conditions, one with air dielectric and the other with 5 mm of tap water layer to assess the oscillations are sustained between the two limits.

In order to interface the oscillator to a PC data acquisition card, the harmonic signal of 13 to 16 MHz generated by each oscillator was first converted to a square wave signal by utilizing a fast comparator MAX 912 and then divided by 8 using a 74LS163 counter to meet the data acquisition card's input frequency range (Advantech PCI-1780 8-ch Counter/Timer Card).

The LC filters are required to prevent any coupling among the oscillators through the common power supply. The array of six oscillators is enclosed in a Faraday cage enclosure each made of mild steel sheet and grounded. This arrangement shields any undesired EM interference between oscillators.

The harmonic signal was converted to TTL signal using dual, high-speed comparators with differential input and consequently six TTL counters were used as 8x frequency dividers. The signal processing part of the system was shrink wrapped to prevent any humidity entering the oscillators, comparators and frequency dividers and the capacitive array PCB was leveled in a deep freezer at $-20°C$ using a custom built frame shown in Figure 7. A flat ribbon cable 1m long interconnected the sensors with the PC and external power supply, and folded flat under the freezer's cover lid.

Our experiments assumed that all capacitive probes in the array face the same conditions, i.e. ice layer and water layer of

Fig. 7. Sensor Leveling prior to the Experiment.

the same height. In case of a small size array this assumption is valid however a sufficient border area around the array should be provided to eliminate potential irregularities due to leading edge or trailing edge boundary effects in certain wind conditions.

To assure a uniform icing buildup, we modified the experimental procedure from [17] and used a paint roller instead of a spray bottle. Three runs were conducted to ensure the uniformity of the ice accretion. The sensor system was tempered at $-20°C$ for two hours before starting the experiment.

V. Results

The experimental setup described above provided data in Figure 8. When the transient response started to settle down, a new wetting cycle was initiated with a total of three cycles. The sharp trough in data plot provides a time reference for each wetting phase which closely corresponds to [17] work with a difference of inverted sign characteristics due to the fact that a frequency is being plotted instead of the capacitance; i.e higher the capacitance lower the frequency.

In line with the above assumption of having all probes facing the same conditions at any time, we introduce a second assumption about the conditions time profile. In this work the icing phenomena is considered to follow a linear time profile for the sake of proof of concept. Other characteristics such as a first-order dynamic response can be used, however, without an accurate real-time ice and water level monitoring system in place, the uncertainty will remain. The objective of our work is not the accuracy or quantitative indicators of ice accretion measurement. In this study, we only assume that each wetting cycle creates a consistent layer of water film across the array. The ice level accounts for 9% increase in the volume. Each consecutive cycle also gets shorter time to settle attributed to the thermal inertia of the accumulated ice layer underneath.

In order to compare and align the data from four oscillators, each frequency was normalized using nominal frequencies acquired when no ice nor water was present. Table II lists the four nominal frequencies along the original frequency and

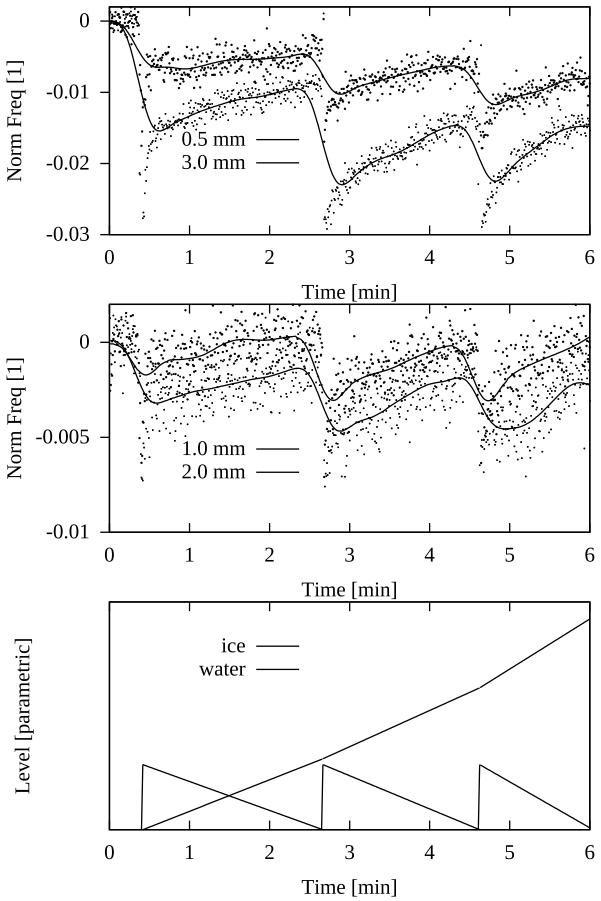

Fig. 8. Back-Shifted Filter Signal Synchronized with the Process.

TABLE II
NOMINAL FREQUENCIES & NORMALIZATION, SAMPLE # 100

gap width	0.5mm f_1	1mm f_2	2mm f_3	3mm f_4
Nominal	1.686 MHz	1.976 MHz	1.907 MHz	1.595 MHz
Measured	1.674 MHz	1.975 MHz	1.899 MHz	1.572 MHz
Normalized	-0.006826	-0.0002940	-0.003981	-0.01406

normalized frequency for #100th sample. The normalization process can be viewed as the sampled data being shifted up or down along the frequency axis and then scaled, the operations that do not affect the linear independence of individual characteristics.

The frequency data were sampled at a rate of 2 samples per second using a DAQ card and the noise was filtered off-line in Matlab using a Butterworth low pass filter with a medium delay of 40 samples. Due to the low sampling frequency we are not confident about the noise origin, however, the lab environment had a large refrigeration equipment running in the vicinity of our setup which suggest a potential 60Hz noise. The signals were also sampled sequentially making the analysis of raw data more challenging, nevertheless, we do include the raw data analysis at the end.

The resulting filtered data sets were then backshifted by 40 samples to align with the original raw data only for the demonstration purposes as illustrated in Figure 8.

To verify the initial hypothesis that an array of planar probes of different spacing parameters can uniquely determine the multiphase phenomena, we propose to use a linear combination of the measured frequencies and their squares similar to the earlier quadratic fit depicted in Figure 1, [17]. (7) reviews this concept including the coefficients $k_1, \ldots, k_8$. One set of eight coefficients is used for determining the ice level ($k_{1i}, \ldots, k_{8i}$.) and another set for the water level $k_{1w}, \ldots, k_{8w}$.

The eight unknown coefficients in (7) can be determined from eight linearly independent equations that correspond to different sample instances. The challenge is to find a set of eight representative samples that will form the eight equations. We took a different approach by using all available samples.

Instead of finding the vector of coefficients **k** from eight linearly independent equations **Fk=h**, we searched for the vector **k** such that **Fk** is as close as possible to **h**, as measured by the square of the Euclidean norm in (4).

$$\begin{aligned} ||\mathbf{Fk}-\mathbf{h}||_2^2 &= (Fk-h)^T(Fk-h) \\ &= k^T F^T Fk - 2h^T Fk + h^T h \end{aligned} \tag{4}$$

Taking the gradient with respect to **k** we obtain (5).

$$\begin{aligned} &\nabla_k(k^T F^T Fk - 2h^T Fk + h^T h) \\ &\quad = \nabla_k k^T F^T Fk - \nabla_k 2h^T Fk + \nabla_k h^T h \\ &\quad = 2F^T Fk - 2F^T h \end{aligned} \tag{5}$$

Setting the gradient expression equal to zero and solving for **k** provides the normal equations in (6).

$$k = \left(F^T F\right)^{-1} F^T h \tag{6}$$

This approach shares some similarities with Artificial Neural Network (ANN) training process, where a training set of input data (frequencies) is presented to ANN along with the desired output (ice layer height and water level height). The difference is that ANN training follows an iterative process of training whereas Least Squares method is not. The solution convergence can be also an issue in ANN's.

We used Matlab to process the Least Squares computations according to (6) and once the coefficients **k** were determined, a test run by evaluating (7) for all samples was performed (j = sample #). The resulting data for both water and ice phase are plotted in Figure 9.

$$h_j = \sum_{N=1}^{4} \left(f_{jN}\right) k_{jN} + \sum_{N=1}^{4} \left(f_{jN}\right)^{\mathbf{2}} k_{j(N+4)} \tag{7}$$

As a result, the ice accretion *measurement* in not significantly impacted by the water phase as was the case of calibrating a sensor using the ice only data. Relatively small deviations are still present in our results, however, these are mainly concentrated around the time when the water layer is being applied to the sensor plane using a paint roller which does not exist in the real world.

We also present a plot on the effects of drifts in offset & parasitic capacitance and dielectric loss (Figure 10). The most common are drifts due to temperature changes or aging. We have subjected the normalized frequency data to a constant offset of 1×10^{-3}, 2×10^{-3} and 3×10^{-3} which represents

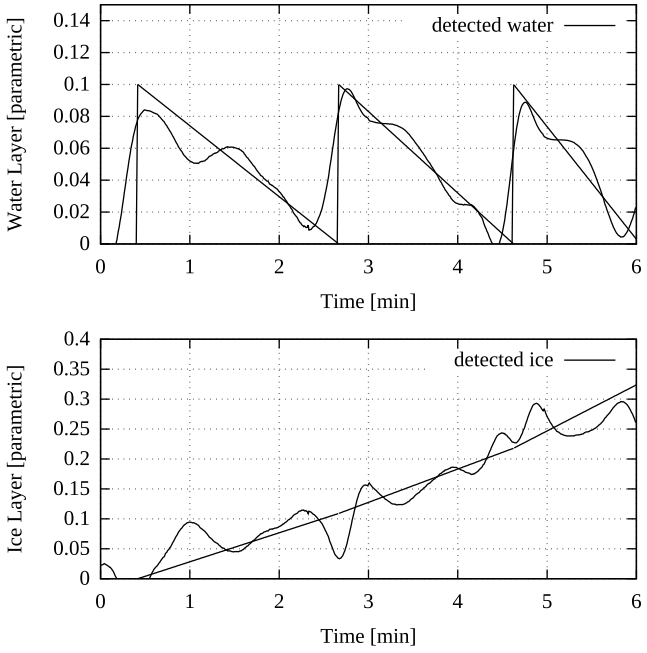

Fig. 9. Detected Ice & Water vs Predictions using Filtered Data.

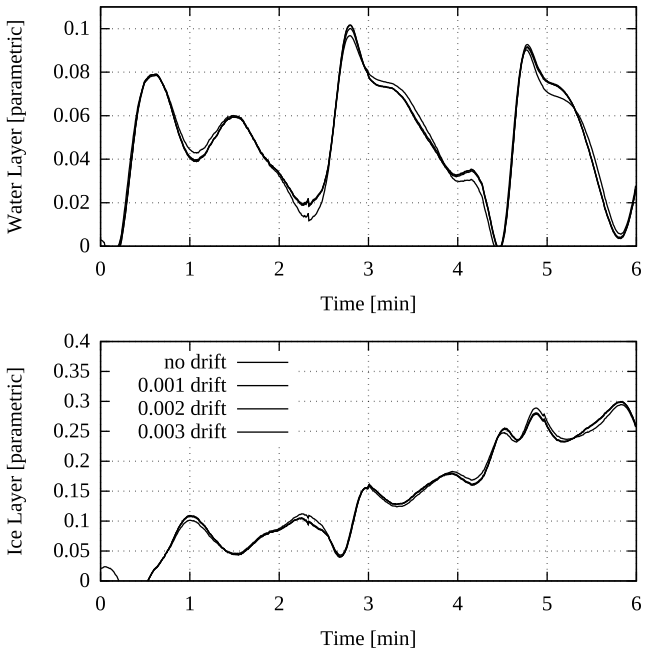

Fig. 10. Detected Ice & Water under Presence of Frequency Drifting.

nearly half of the total frequency range in '1mm' and '2mm' sensors. Yet the effect on the output is found insignificant in view of the other inaccuracies. A more detailed analysis would be needed in the future research including both absolute and relative data drifts.

The raw data analysis results are plotted in Fig 11 for completeness. The water and ice detection is not as close to the predicted profiles obtained in the filtered data analysis showed, however the approximate tendencies are clear without the order of magnitude errors we experienced before.

This scope-limited study also revealed where we need to focus in the future development. As the next step,

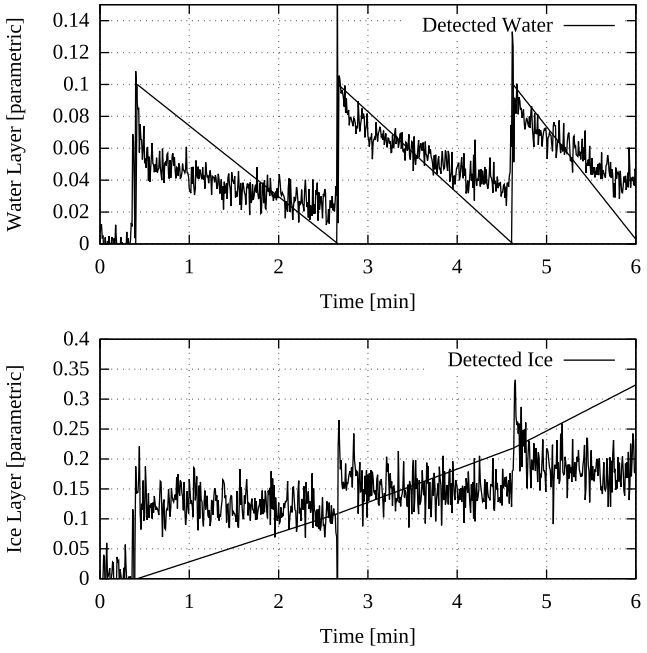

Fig. 11. Detected Ice & Water vs Predictions using Raw Data.

this reaserch will incorporate a calibration system that will quantify the sensitivity and robustness of our system. A more robust drift-free signal conversion techniques will also be studied.

VI. Conclusion

The presented work focused on development of a marine icing monitoring system under the real conditions of multiphase phenomena as the current monitoring systems do not consider the unique conditions. We have developed a novel method of utilizing an array of capacitive probes of different aspect ratio and thus a different penetration depth to be a candidate for multiphase phenomena sensing. FEM analysis was conducted to provide a theoretical proof of the novel approach. Then an experimental setup was developed to validate the proposed approach. The objective of our experiments was to prove the ability of our system to recognize the multiphase phenomena.

Instead of the traditional 'quantitative calibration' we selected a 'qualitative calibration' approach which only assumed three *identical & uniform* layers of water film applied to the sensor plane at each wetting cycle. Least Squares equations were solved to find a correlation among the array capacitances (measured as frequency) and the water & ice layer height represented parametrically. The experimental results confirmed our predictions which gives our novel approach the necessary backing to be developed further.

Acknowledgment

The authors would like to acknowledge and thank Mitacs Canada and Equinor ASA (formerly Statoil) for providing research funding to this project and to the Libyan Ministry of Education for providing a postgraduate fellowship to the first author. Without the contributions this work would not be possible.

REFERENCES

[1] S. M. Fikke *et al.*, *COST 727: Atmospheric Icing on Structures: Measurements and Data Collection on Icing: State of the Art*. Zürich, Switzerland: MeteoSwiss, 2006.

[2] R. Cattin and U. Heikkil, "Evaluation of ice detection systems for wind turbines," Weather Forecasts-Renew. Energies-Air, Climate-Environ. IT, METEOTEST, Bern, Switzerland, VGB Res. Project 392, 2016.

[3] S. R. Dehghani, Y. S. Muzychka, and G. F. Naterer, "A finite difference solution for freezing brine on cold substrates of spongy ice," *Int. J. Heat Fluid Flow*, vol. 69, pp. 174–184, Feb. 2018.

[4] A. Dehghani-Sanij, Y. S. Muzychka, and G. F. Naterer, "Analysis of ice accretion on vertical surfaces of marine vessels and structures in arctic conditions," in *Proc. OMAE*, St. John's, NF, Canada, 2015, Art. no. V007T06A056.

[5] A. Fazelpour, S. R. Dehghani, V. Masek, and Y. S. Muzychka, "Ice load measurements on known structures using image processing methods," *World Acad. Sci., Eng. Technol. Int. J. Elect. Comput. Eng.*, vol. 11, no. 8, pp. 829–832, Jun. 2017.

[6] A. Fazelpour, S. R. Dehghani, V. Masek, and Y. S. Muzychka, "Effect of ambient conditions on infrared ice thickness measurement," in *Proc. IEEE NECEC Conf.*, Nov. 2016.

[7] A. Fazelpour, S. R. Dehghani, V. Masek, and Y. S. Muzychka, "Infrared image analysis for estimation of ice load on structures," in *Proc. Offshore Technol. Conf.*, 2016, pp. 1–11, Paper OTC-27409-MS.

[8] T. Rashid, H. A. Khawaja, and K. Edvardsen, "Measuring thickness of marine ice using IR thermography," *Cold Regions Sci. Technol.*, vol. 158, pp. 221–229, Feb. 2019. doi: 10.1016/j.coldregions.2018.08.025.

[9] M. Neumayer, T. Bretterklieber, and M. Flatscher, "Signal processing for capacitive ice sensing: Electrode topology and algorithm design," *IEEE Trans. Instrum. Meas.*, vol. 68, no. 5, pp. 1458–1466, May 2019.

[10] *The Ice Load Surveillance Sensor IceMonitor, Product Sheet*, Combitech AB, Växjö, Sweden, 2013.

[11] *Goodrich Ice Detector Models 0871LH1*, UTC Aerosp. Syst., Burnsville, MN, USA, 2013.

[12] *T40 Series of Icing Rate Sensors, User Guide*, HoloOptics, Stockholm, Sweden, 2008.

[13] *Ice Meister Model 9734—Industrial Ice Detecting Sensor System*, New Avionics Corp., Fort Lauderdale, FL, USA, 2015.

[14] *IDS-20 Product Information*, SOMMER Messtechnik, Koblach, Austria, Nov. 2016.

[15] X. Zhi, H. C. Cho, B. Wang, C. H. Ahn, H. S. Moon, and J. S. Go, "Development of a capacitive ice sensor to measure ice growth in real time," *Sensors*, vol. 15, pp. 6688–6698, Mar. 2015.

[16] J. S. Go, M. Y. Ha, C. Son, and J. K. Min, "Ice thickness measurement sensor," EP Patent 2 918 965 B1, Feb. 17, 2015.

[17] C. Ezeoru, "Marine icing sensor design using capacitive techniques," M.S. thesis, Memorial Univ. Newfoundland, St. John's, NL, Canada, Aug. 2016. [Online]. Available: https://research.library.mun.ca/12492/

[18] L. K. Baxter, *Capacitive Sensors: Design and Applications*. New York, NY, USA: IEEE Press, 1997.

[19] K. I. Arshak, D. Morris, A. Arshak, O. Korostynska, and E. Jafer, "Development of a wireless pressure measurement system using interdigitated capacitors," *IEEE Sensors J.*, vol. 7, no. 1, pp. 122–129, Jan. 2007.

[20] Y. Gong, H. Y. Zhu, and N. Li, "Research on coplanar capacitive sensor design for film thickness measurement," *Adv. Mater. Res.*, vols. 945–949, pp. 2030–2036, Jun. 2014.

[21] T. Chen and N. Bowler, "Analysis of a concentric coplanar capacitive sensor for nondestructive evaluation of multi-layered dielectric structures," *IEEE Trans. Dielectr. Electr. Insul.*, vol. 17, no. 4, pp. 1307–1318, Aug. 2010.

[22] S. Malik, M. Ahmad, S. Laxmeesha, T. Islam, and M. S. Baghini, "Impedance-to-time converter circuit for leaky capacitive sensors with small offset capacitance," *IEEE Sensors Lett.*, vol. 3, no. 7, Jul. 2019, Art. no. 7001004.

[23] A. Risos, N. Long, A. Hunze, and G. Gouws, "A 3D Faraday shield for interdigitated dielectrometry sensors and its effect on capacitance," *Sensors*, vol. 17, no. 1, p. 77, 2017.

[24] A. Risos, N. Long, A. Hunze, and G. Gouws, "Interdigitated sensors: A design principle for accurately measuring the permittivity of industrial oils," *IEEE Sensors J.*, vol. 17, no. 19, pp. 6232–6239, Oct. 2017.

[25] A. Risos, "Interdigitated sensors: The next generation 'sensing permittivity and conductivity of oils—Unaffected by temperature,"' *IEEE Sensors J.*, vol. 18, no. 9, pp. 3661–3668, May 2018.

[26] A. Risos and G. Gouws, "*In-situ* aging monitoring of transformer oil via the relative permittivity and DC conductivity using novel interdigitated dielectrometry sensors (IDS)," *Sens. Actuators, B. Chem.*, vol. 287, pp. 602–610, May 2019.

[27] T. Chen, J. Song, J. R. Bowler, and N. Bowler, "Analysis of a concentric coplanar capacitive sensor using a spectral domain approach," in *Proc. AIP Conf.*, vol. 1335, 2011, p. 1647. doi: 10.1063/1.3592126.

[28] N. Bowler and T. Chen, "Concentric coplanar capacitive sensor system with quantitative model," U.S. Patent 8 791 707 B2, Jul. 29, 2014.

[29] D. Wang, *FDC1004: Basics of Capacitive Sensing and Applications*, Texas Instrum., Dallas, TX, USA, 2014.

[30] W.-C. Heerens, "Application of capacitance techniques in sensor design," *J. Phys. E, Sci. Instrum.*, vol. 19, no. 11, pp. 897–906, 1986.

[31] J. Ortiz and V. Masek, "Cyclonic capacitive sensor for multiphase composition measurement," *Sens. Transducers*, vol. 191, no. 8, pp. 1–11, 2015.

Abdulrazak Elzaidi received the bachelor's degree in control engineering, and the master's degree in mechatronics engineering from the Faculty of Computer Technology, Tripoli University, Libya, in 1999 and 2009, respectively. He is currently pursuing the Ph.D. degree in electrical engineering with the Faculty of Engineering and Applied Science, Memorial University of Newfoundland, Canada.

His research includes sensors for multiphase phenomena and marine icing.

Vlastimil Masek received the Ph.D. degree in mechanical and control engineering from the University of Electro-Communications, Tokyo, Japan, in 1999.

He is currently an Associate Professor with the Department of Electrical and Computer Engineering, Memorial University of Newfoundland, St. John's, Canada. He currently supervises research projects in the area of control and instrumentation with target applications in oil and gas, offshore industries, wide area oceanography, and the environment protection.

Prof. Masek is a registered Professional Engineer in the Province of Newfoundland and Labrador.

Yuri Muzychka received the Ph.D. degree in mechanical engineering from the University of Waterloo, Waterloo, ON, Canada, in 1999.

He is currently a Professor of Mechanical Engineering with the Memorial University of Newfoundland, St. Johns, NL, Canada. He has published over 200 papers in refereed journals and conference proceedings in these areas. His current research interests include the development of robust models for characterizing transport phenomena using the fundamental theory, marine icing, electronics cooling, and energy systems.

Prof. Muzychka is a registered Professional Engineer and a member of the American Institute for Aeronautics and Astronautics, and a Fellow of the American Society of Mechanical Engineers.